Journal of Statistical Physics, Vol. 78, Nos. 3/4, 1995

Numerical Results for the Three-State Critical Potts Model on Finite Rectangular Lattices

M. J. O'Rourke,[1] R. J. Baxter,[2] and V. V. Bazhanov[2]

Received June 6, 1994

Partition functions for the three-state critical Potts model on finite square lattices and for a variety of boundary conditions are presented. The distribution of their zeros in the complex plane of the spectral variable is examined and is compared to the expected infinite-lattice result. The partition functions are then used to test the finite-size scaling predictions of conformal and modular invariance.

KEY WORDS: Statistical mechanics; lattice statistics; solvable models; three-state Potts model; zeros of the partition function; conformal invariance; modular invariance.

1. INTRODUCTION

The location in the complex plane of the zeros of the partition function of a statistical mechanical model has been a much studied area since the publication of Lee and Yang's circle theorem for the Ising model in 1952.[1] For the Potts model[2,3] numerical studies of the location of the zeros have been carried out in, for example, refs. 4–7.

Baxter has studied the zeros of the partition function of the zero-temperature antiferromagnetic q-state Potts model on the triangular lattice, expressing the partition function Z as a polynomial in the variable q. Martin *et al.* considered the three-state Potts model on triangular and square

[1] Theoretical Physics, I.A.S., Australian National University, Canberra, A.C.T. 0200, Australia.

[2] Theoretical Physics, I.A.S., and School of Mathematical Sciences, Australian National University, Canberra, A.C.T. 0200, Australia.

0022-4715/95/0200-0665$07.50/0

lattices in two and three dimensions, expressing the partition functions as polynomials in a temperature-like variable. Here we study the square-lattice three-state Potts model at criticality, expressing Z as a polynomial in a variable z related to the anisotropy (often called the spectral parameter) of the model.

As the partition functions can be expressed as polynomials, they are determined up to a constant multiple by the location of their zeros. In the thermodynamic limit, we expect[8] the zeros to accumulate on lines dividing the complex z plane into domains, the free energy having a different analytical form in each domain.

A variety of boundary conditions have been considered by us, including cylindrical, toroidal, and skew-toroidal. It is expected that the distribution of zeros of a finite system with toroidal boundary conditions will approximate better the distribution in the thermodynamic limit than either systems with cylindrical or fixed boundary conditions, and this behavior was observed.

At criticality, the Potts model is solvable by a Bethe ansatz.[9-11] While this gives explicit formulas for the infinite system, the results for a finite lattice are still extremely complicated. Rather than use these, we have calculated Z directly (using edge transfer matrices to build up the lattice one edge at a time). Part of our motivation is to better understand the results of the Bethe ansatz by studying the analytic properties of the partition function in the complex z plane.

We are also able to test the finite-size scaling predictions of conformal and modular invariance for a critical system. One expects the partition function for a finite $L \times M$ lattice, Z_{LM}, to be related to the free energy per site of the infinite system f by the relation[12]

$$\ln Z_{LM} = -2LMf/kT + \ln Z(q) + \text{correction terms} \tag{1.1}$$

where k is Boltzmann's constant, T is the temperature of the system, and $Z(q)$, defined in Section 3, is the modular invariant partition function of the system, which characterizes the finite-size corrections for the system. The correction terms approach zero as $L, M \to \infty$.

Given the relatively small sizes of the lattices considered, we found this relationship to hold to a remarkable degree of accuracy. In particular, for a spatially isotropic model on an $L \times L$ lattice, for which $\ln Z(q) \sim 1$, the correction terms appear to approach zero as $1/L$, with a very small (~ 0.04) numerical coefficient.

2. PARTITION FUNCTIONS AND EXACT SOLUTION

2.1. Toroidal Boundary Conditions

Consider the "$L \times M$" rectangular lattice $\mathscr{L}_{LM}$, rotated through 45 deg, shown in Fig. 1. It has $2M$ rows, each containing L sites, so there is a total of $2LM$ sites. Spin variables σ_i live on each site of the lattice, and we allow each of them to take on the integer values 0,..., $N-1$. Nearest-neighbor spins interact along the bonds of the lattice, with Boltzmann weights $W(\sigma_i - \sigma_j)$ in the SW → NE direction, and $\bar{W}(\sigma_i - \sigma_j)$ in the SE → NW direction, indicated also in Fig. 1. (Differences between spins are interpreted *modulo N*.)

We assume first toroidal boundary conditions on the lattice. Thus in each row we identify the first and last spins, so that $\sigma_1 = \sigma_{L+1}$, where σ_1, σ_{L+1} are the first and last spins in the row, respectively, and in each column we identify the top with the bottom spin of that column, $\sigma_i^{(1)} = \sigma_i^{(M+1)}$, where $\sigma_i^{(1)}, \sigma_i^{(M+1)}$ are the bottom and top spins in the ith column, respectively.

The partition function for the model on an $L \times M$ lattice can be written as

$$Z_{LM} = \sum_{\{\sigma\}} \prod_{\langle i,j \rangle} W(\sigma_i - \sigma_j) \prod_{\langle i,k \rangle} \bar{W}(\sigma_i - \sigma_k) \tag{2.1}$$

where the sum is over all values 0 to $N-1$ of all the spins σ_i, and the products are over all SW → NE edges $\langle i, j \rangle$ and all SE → NW edges $\langle i, k \rangle$.

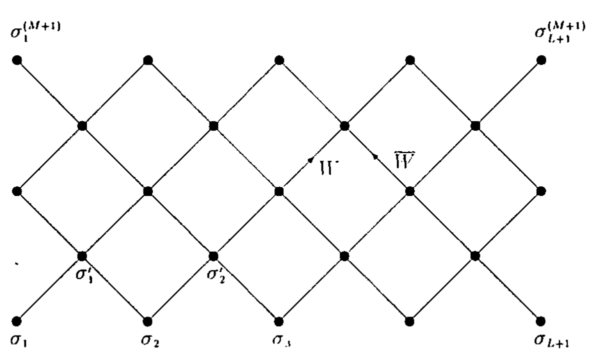

Fig. 1. The square lattice $\mathscr{L}_{LM}$ with L sites per row and $M = 2$. The weight functions W and $\bar{W}$ are indicated.

This definition suits a large class of models, including the chiral Potts model.[13, 14] In this paper we consider the critical ($N=3$)-state Potts model, which is a particular (critical) case of the chiral Potts model. It also coincides with the $\mathbf{Z}_3$ Fateev–Zamolodchikov model[15] and with the $N=3$ critical Kashiwara–Miwa model.[16]

We parametrize the Boltzmann weights as

$$W(0) = (1+x)/x \tag{2.2a}$$

$$W(1) = W(2) = 1 \tag{2.2b}$$

$$\bar{W}(0) = 1 + 3x \tag{2.2c}$$

$$\bar{W}(1) = \bar{W}(2) = 1 \tag{2.2d}$$

where x can be considered to be an anisotropy parameter.

From (2.1), $Z_{LM}(x)$ will be a Laurent polynomial in x with positive integer coefficients, which we have calculated for a variety of lattices.

For the calculations, we actually used edge transfer matrices[17] instead of (2.1) to calculate the partition function, calculating the polynomials using Fortran and modular arithmetic.[18] When considering the zeros of a polynomial, it is important to evaluate the coefficients exactly, as the location of the zeros can be sensitive to errors in the coefficients.

We found the length of the largest coefficient in the polynomials to increase exponentially with the size of the lattice, and for the 6×6 lattice, the longest coefficient was already an integer of order 10^{66}. A rotation of the lattice through 90 deg is equivalent to replacing x by $1/3x$, so for toroidal boundary conditions, Z_{LM} must be a polynomial in $y = 3x + 1/x$. Expressing the partition function in terms of y halves the degree of the polynomial, and approximately halves the length of the coefficients, both of which make it easier to handle the polynomial. The partition functions for 1×1 up to 5×5 lattices are presented in the appendix in terms of the variable y.

The free energy of the Potts model at criticality can be found either by its Temperley–Lieb equivalence to an ice-type model as in refs. 9 and 17 or by the inversion relation method.[8] Following ref. 8, we introduce the variable μ, where $2\cos\mu = \sqrt{N}$, so $\mu = \pi/6$. We then reparametrize the anisotropy variable x in terms of the spectral parameter v,

$$x = \frac{1}{\sqrt{3}} \frac{\sin(\mu - v)}{\sin v} \tag{2.3}$$

The Boltzmann weights are then

$$W(0)=\frac{\sin(\mu+v)}{\sin(\mu-v)} \tag{2.4}$$

$$\bar{W}(0)=\frac{\sin(2\mu-v)}{\sin v} \tag{2.5}$$

The others remain unchanged. Regarding v as a variable, we denote the partition function per site for a finite lattice as $\kappa_{LM}(v)=(Z_{LM})^{1/2LM}$, and for the infinite lattice

$$\kappa(v)=\lim_{L,M\to\infty}\kappa_{LM}(v) \tag{2.6}$$

where the limit is taken through large values of both L and M.

In ref. 8 a number of relations for $\kappa(v)$ are given, including the inversion, periodicity, and crossing symmetry relations. The latter two are

$$\kappa(v)=\kappa(\pi+v) \tag{2.7}$$

$$\kappa(v)=\kappa(\mu-v) \tag{2.8}$$

To match the normalization of the weights (2.4) and (2.5) with those used in ref. 8, we should take the constant ρ_0 therein to be

$$\rho_0=\frac{\sin\mu\sin 2\mu}{\sin v\sin(\mu-v)} \tag{2.9}$$

The inversion relations for $\kappa(v)$ then read[8]

$$\kappa(v)\,\kappa_{\mathrm{ac}}(-v)=\rho_0^2\sin(\mu+v)\sin(\mu-v)/\sin^2\mu \tag{2.10a}$$

$$\kappa(v)\,\kappa_{\mathrm{ac}}(2\mu-v)=\rho_0^2\sin v\sin(2\mu-v)/\sin^2\mu \tag{2.10b}$$

$$\kappa(v)\,\kappa_{\mathrm{ac}}(\pi-v)=-\rho_0^2\sin(\mu-v)\sin(\mu+v)/\sin^2\mu \tag{2.10c}$$

$$\kappa(v)\,\kappa_{\mathrm{ac}}(\pi+2\mu-v)=-\rho_0^2\sin v\sin(2\mu-v)/\sin^2\mu \tag{2.10d}$$

where $\kappa_{\mathrm{ac}}(v)$ is the analytic continuation of $\kappa(v)$ through the point $v=0$, defined in ref. 8. To get the free energy from the inversion relations, one uses Eqs. (2.10a) and (2.10b) when $0<\mathrm{Re}(v)<\mu$, (2.10b) and (2.10c) when $\mu<\mathrm{Re}(v)<\pi/2$, (2.10c) and (2.10d) when $\pi/2<\mathrm{Re}(v)<\mu+\pi/2$, and Eqs. (2.10d), (2.10a), and (2.7) for $\mu+\pi/2<\mathrm{Re}(v)<\pi$.

This divides the complex v plane into four regions, in each of which $\kappa(v)$ has a different analytical form. The physical regime is when $0<\mathrm{Re}(v)<\mu$, where all the Boltzmann weights are real and positive. The expressions for $\kappa(v)$ in each of the regions can be found from the appropriate inversion relations above with some analyticity assumptions[8] on $\kappa(v)$, and the results are presented here for completeness.

(i) For $0<\mathrm{Re}(v)<\mu$:

$$\ln \kappa(v)=\ln \rho_0+2\int_{-\infty}^{\infty} \frac{\cosh(\pi-2\mu)t \sinh vt \sinh(\mu-v)t}{t \sinh \pi t \cosh \mu t}\,dt \qquad (2.11\mathrm{a})$$

(ii) $\mu<\mathrm{Re}(v)<\frac{1}{2}\pi$:

$$\ln \kappa(v)=\ln \rho_0+2\int_{-\infty}^{\infty} \frac{\phi(\mu, v, t) \sinh(v-\mu)\,t}{t \sinh \pi t \sinh(\pi-2\mu)t}\,dt \qquad (2.11\mathrm{b})$$

where

$$\phi(\mu, v, t)=\sinh(\pi-\mu)\,t \sinh(\pi-2\mu-v)\,t+\sinh \mu t \sinh(v-2\mu)\,t \qquad (2.11\mathrm{c})$$

(iii) $\frac{1}{2}\pi<\mathrm{Re}(v)<\mu+\frac{1}{2}\pi$:

$$\ln \kappa(v)=\ln \rho_0+\int_{-\infty}^{\infty} \frac{\cosh \mu t \cosh(\pi-2\mu)t-\cosh 2\mu t \cosh(2v-\pi-\mu)t}{t \sinh \pi t \cosh \mu t}\,dt \qquad (2.11\mathrm{d})$$

(iv) $\mu+\frac{1}{2}\pi<\mathrm{Re}(v)<\pi$:

$$\ln \kappa(v)=\ln \rho_0+2\int_{-\infty}^{\infty} \frac{\phi(\mu, \pi+\mu-v, t) \sinh(\pi-v)\,t}{t \sinh \pi t \sinh(\pi-2\mu)t}\,dt \qquad (2.11\mathrm{e})$$

Equation (2.7) is used to find in $\ln \kappa(v)$ outside the range $0<v<\pi$. Since $\mu=\pi/6$ is a rational fraction of π, we can reduce these integrals to infinite series. For the physical regime, Eq. (2.11a) thus gives

$$\ln \kappa(v)=\frac{1}{2}\ln 3+\frac{4}{3\pi}\sum_{n=1}^{\infty}\frac{\sin 6v(2n-1)}{(2n-1)^2}+\frac{2}{\pi}(\mu-2v)\ln \cot 3v$$
$$+\ln \frac{\sin(\mu+v)\sin(2\mu-v)}{\sin(\mu-v)\sin v}+\frac{1}{3}\ln[\tan v \tan(\mu-v)] \qquad (2.12)$$

In the thermodynamic limit, we expect the zeros of the partition function to lie on the boundaries between these phases, which is when $\mathrm{Re}(v)=0$, μ, $\pi/2$, or $\mu+\pi/2$.

We introduce a new variable

$$z=e^{2iv}=\frac{(1-\omega^2)x-\omega^2}{(1-\omega^2)x+1} \qquad (2.13)$$

and have plotted the zeros for the finite lattices in the z plane. Then the boundaries between the phases are the rays $\arg(z) = 0$, $\pi/3$, π, or $4\pi/3$, or equivalently the line $\mathrm{Re}(x) = -1/2$ and the circle $[\mathrm{Re}(x) + 1/3]^2 + \mathrm{Im}(x)^2 = 1/9$. These rays in the z plane are indicated in Fig. 2.

The zeros in the z plane for the 4×4, 5×5, and 6×6 lattices are shown in Figs. 2–4, respectively. They are beginning to fall on the expected rays, with some scatter at the ends of each ray. Also note the line of zeros for the 5×5 lattice with arguments of approximately $\pm 2\pi/3$. For the lattices we looked at (1×1 through 6×6), these occurred when L and M were both odd.

We can verify the calculation in ref. 8 of the density of zeros lying on each contour of the phase diagram. According to Eqs. (5.15) of ref. 8, one would expect to find for an $L \times M$ lattice the fraction $(\pi - 3\mu)/(\pi - 2\mu) = 3/4$ of the zeros on the rays $\arg z = 0$ and $\pi/3$, and the other $\mu/(\pi - 2\mu) = 1/4$ of the zeros on the rays $\arg z = \pi$ and $4\pi/3$. That this is the case can be verified from the included graphs, and is most obvious in Fig. 2, which shows the distribution of zeros for the 4×4 lattice partition function, and the rays on which we would expect the zeros to lie in the thermodynamic limit. There are 64 zeros, with 8 of them "on" each of the rays $\arg z = \pi$ and $4\pi/3$, and 24 of them "on" each of the remaining two rays, as expected.

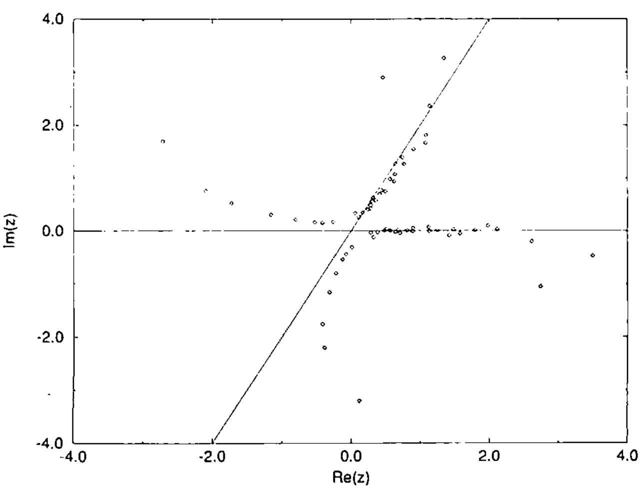

Fig. 2. Zeros of the partition function for 4×4 lattice, showing the lines on which the zeros are expected to accumulate in the infinite-lattice limit.

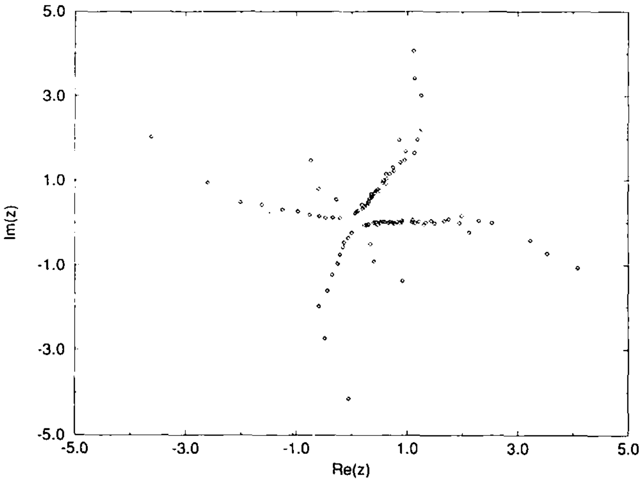

Fig. 3. Zeros of the partition function for the 5×5 lattice.

2.2. Skew-Toroidal Boundary Conditions

The effect of introducing skewed boundary conditions onto the lattice was also investigated. For an $L \times M$ lattice with toroidal boundary conditions, we identify the first and last spins in each row and the top and bottom spins in each column. If we skew the boundary conditions, we

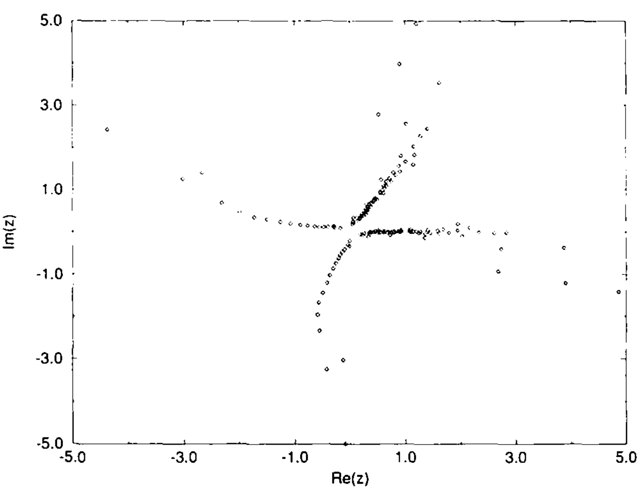

Fig. 4. Zeros of the partition function for the 6×6 lattice.

instead identify $\sigma_1 = \sigma_{L+1} + h$, $\sigma_i^{(1)} = \sigma_i^{(M+1)} + v$, where h and v are the horizontal and vertical skewing parameters, σ_1, σ_{L+1} are the first and last spins in a horizontal row, and $\sigma_i^{(1)}$, $\sigma_i^{(M+1)}$ are the bottom and top spins in column i. We denote the partition function of the model on the $L \times M$ lattice with skewing parameters h and v as Z_{LM}^{hv}. We can restrict without loss of generality the skewing parameters to take the values 0, 1, 2, so in general we will expect nine partition functions with skewed boundary conditions.

These nine functions quickly reduce to five, and only four for a square lattice, when symmetries of the model on the lattice are taken into account. From Eqs. (2.2a)–(2.2d), replacing x by $1/3x$ is equivalent to interchanging $W(n)$ with $\bar{W}(n)$. Reflecting the lattice horizontally or vertically, we thus get

$$Z_{LM}^{h,v}(x) = Z_{LM}^{-h,v}\left(\frac{1}{3x}\right) = Z_{LM}^{h,-v}\left(\frac{1}{3x}\right) \tag{2.14}$$

and so we are just left with the following five partition functions:

$$\begin{aligned} Z_{LM}^{00}(x) &= Z_{LM}(x) \\ Z_{LM}^{01}(x) &= Z_{LM}^{02}(x) \\ Z_{LM}^{10}(x) &= Z_{LM}^{20}(x) \\ Z_{LM}^{11}(x) &= Z_{LM}^{22}(x) \\ Z_{LM}^{12}(x) &= Z_{LM}^{21}(x) \end{aligned} \tag{2.15}$$

Rotating the lattice through 90 deg is equivalent to interchanging $W(n)$ with $\bar{W}(n)$ and L with M. This gives the symmetry relation

$$Z_{LM}^{h,v}(x) = Z_{ML}^{-v,h}\left(\frac{1}{3x}\right) \tag{2.16}$$

which, on a square lattice, gives us the relationship

$$Z_{LL}^{01}(x) = Z_{LL}^{10}(x) \tag{2.17}$$

and so there are only the four different partition functions on a square lattice.

Finally we note the relation following from the self-duality property of the model

$$Z_{LM}^{00}(x) = Z_{LM}^{01}(x) + Z_{LM}^{10}(x) + Z_{LM}^{11}(x) + Z_{LM}^{12}(x) \tag{2.18}$$

and this was verified for all the partition functions generated.

Guided by the Ising model case [Eq. (5.2) of chapter IV of ref. 19], one may expect that certain linear combinations of these partition functions have zeros located on some simple curves (even for finite L and M). This does not seem to be the case for the three-state Potts model, we were unable to find any linear combination whose zeros lay on simple contours and remained there as the lattice size was increased.

3. FINITE-SIZE CORRECTIONS

3.1. Conformal and Modular Invariance

The partition functions we have calculated can be used to test the predictions of finite-size corrections due to conformal and modular invariance. Many reviews of these subjects exist,[12, 20-23] and only a summary of the necessary results will be presented here.

At criticality, various observables of a statistical mechanical system are believed to be invariant under scaling and conformal transformations. This assumption, which originally led to predictions of relationships between the critical exponents,[24] has been developed into a classification of universality classes of the critical behavior for two-dimensional systems (determined by a parameter c, the central charge of the Virasoro algebra associated with the model)[25] and more recently into a classification of the modular invariant partition functions on a torus.[26]

It was shown in ref. 27 that for a statistical mechanical system with a Hermitian transfer matrix, corresponding to a unitary conformal field theory, if $c < 1$, then c is restricted to take on the values

$$c = 1 - \frac{6}{h(h-1)} \tag{3.1}$$

where $h = 4, 5, 6, \ldots$.

Modular invariance predicts the leading corrections to the partition function should take the form (1.1), where Z_{LM} is the partition function on an $L \times M$ lattice, f is the free energy per site in the thermodynamic limit, and $Z(q)$ describes the leading finite-size corrections in the limit of L, M large, with the ratio L/M fixed. Here q is the modular parameter, given by[20]

$$q = e^{2\pi i \tau}, \qquad \tau = e^{i(\pi - \theta)} L/M \tag{3.2}$$

where $\theta = 6v$ is the spatial anisotropy of the model.

One requires $Z(q)$ to be invariant under the action of the modular group, which maps a torus formed by identifying sides of a parallelogram in the complex plane with vertices 0, 1, τ, and $1+\tau$ onto itself. The modular group acts through the generators T and S, where

$$T:\quad \tau \to 1+\tau \tag{3.3a}$$

$$S:\quad \tau \to -\tau^{-1} \tag{3.3b}$$

Note that the rotational symmetry $x \to 1/3x$ of Z_{LM} corresponds to (3.3b).

These requirements place very stringent constraints on the form of $Z(q)$, and in fact lead to a complete classification of all possible modular invariant partition functions for $c<1$ theories, which are labeled by the A, D, and E Lie algebras.[26]

The three-state Potts model is related to the D_4 minimal conformal field theory[26] with $c=4/5$, $h=6$.[28] The corresponding modular invariant partition function reads

$$Z(q) = |\chi_{1,1}(q)+\chi_{4,1}(q)|^2 + |\chi_{2,1}(q)+\chi_{3,1}(q)|^2 + 2\,|\chi_{3,3}(q)|^2 + 2\,|\chi_{4,3}(q)|^2 \tag{3.4}$$

where $\chi_{r,s}$ is the character of the representation of the Virasoro algebra, given by

$$\chi_{r,s} = q^{-c/24} \prod_{n=1}^{\infty} (1-q^n)^{-1} \times \sum_{n=-\infty}^{\infty} \left\{ q^{\{[2h(h-1)n+hr-(h-1)s]^2-1\}/4h(h-1)} - q^{\{[2h(h-1)n+hr+(h-1)s]^2-1\}/4h(h-1)} \right\} \tag{3.5}$$

3.2. Numerical Results

In this section, we shall verify the predictions of modular invariance by numerically evaluating the correction terms in (1.1) for various lattice sizes and demonstrating that they vanish as the lattice size increases. Writing the correction terms as C_{LM}, we can write (1.1) as

$$\ln Z_{LM}(v) = -2LMf/kT + \ln Z(q) + C_{LM} \tag{3.6}$$

and we expect that

$$C_{LM} \to 0 \qquad \text{as} \quad L, M \to \infty \tag{3.7}$$

It is computationally easier to evaluate the partition function Z_{LM} numerically for a particular value of x than it is to evaluate the entire

Table I. Correction Terms C_{LM} for the Isotropic Model

M	$L=1$	2	3	4	5	6	7	8	9
1	0.0341	0.0852	0.1580	0.2342	0.3078	0.3781	0.4458	0.5119	0.5771
2	0.0852	0.0194	0.0251	0.0360	0.0479	0.0603	0.0728	0.0852	0.0974
3	0.1580	0.0251	0.0132	0.0140	0.0170	0.0206	0.0242	0.0279	0.0317
4	0.2342	0.0360	0.0140	0.0099	0.0098	0.0110	0.0124	0.0139	0.0154
5	0.3078	0.0479	0.0170	0.0098	0.0079	0.0077	0.0082	0.0089	0.0096
6	0.3781	0.0603	0.0206	0.0110	0.0077	0.0066	0.0064	0.0066	0.0070
7	0.4458	0.0728	0.0242	0.0124	0.0082	0.0064	0.0057	0.0055	0.0056
8	0.5119	0.0852	0.0279	0.0139	0.0088	0.0066	0.0055	0.0050	0.0049
9	0.5771	0.0974	0.0317	0.0154	0.0096	0.0070	0.0056	0.0049	0.0045

polynomial, and so for these calculations we are able to use larger lattice sizes than in Section 2. Here, we present results on up to 9×9 lattices.

For the numerical studies, we considered an isotropic ($\theta = \pi/2$) and a particular anisotropic ($\theta = \pi/4$) case of the model. From (2.12) and (3.2) we have

$$\text{(i)} \quad \theta = \pi/2, \quad q = \exp(-2\pi L/M), \quad f/kT = 2.0702 \tag{3.8a}$$

$$\text{(ii)} \quad \theta = \pi/4, \quad q = \exp[-\sqrt{2}\,\pi(1+i)L/M], \quad f/kT = 2.3150 \tag{3.8b}$$

where (i) and (ii) correspond to the isotropic and anisotropic cases, respectively. Using these and the numerical values of Z_{LM}, we calculated C_{LM}. They are given in Tables I and II for all $L \times M$ lattices with $1 \leqslant L, M \leqslant 9$. The correction terms are close to zero as expected, and vanish as the lattice size increases in both directions.

Table II. Correction Terms C_{LM} for the Anisotropic Model

M	$L=1$	2	3	4	5	6	7	8	9
1	0.0256	0.0266	0.0385	0.0505	0.0625	0.0746	0.0867	0.0988	0.1111
2	0.0266	−0.0090	0.0141	0.0109	0.0116	0.0115	0.0110	0.0103	0.0095
3	0.0385	0.0141	−0.0042	0.0085	0.0086	0.0077	0.0076	0.0074	0.0069
4	0.0505	0.0109	0.0085	0.0001	0.0057	0.0070	0.0065	0.0062	0.0060
5	0.0625	0.0116	0.0086	0.0057	0.0021	0.0045	0.0057	0.0056	0.0053
6	0.0746	0.0115	0.0077	0.0070	0.0045	0.0028	0.0039	0.0047	0.0048
7	0.0867	0.0110	0.0076	0.0065	0.0056	0.0039	0.0029	0.0035	0.0040
8	0.0988	0.0103	0.0074	0.0062	0.0056	0.0047	0.0035	0.0029	0.0031
9	0.1111	0.0095	0.0070	0.0060	0.0053	0.0048	0.0040	0.0031	0.0028

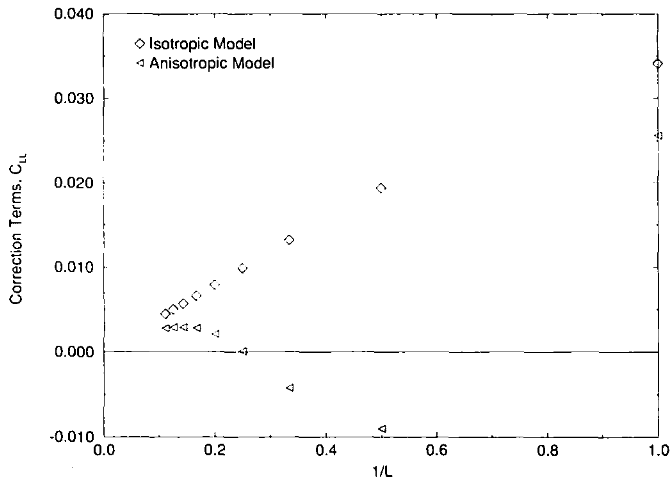

Fig. 5. Next-order corrections to the modular invariant partition function. Top: isotropic model; below: anisotropic model.

We next restricted our attention to just the square $L \times L$ lattices. In this case, we have for the isotropic model (i) $\ln Z(q) = 1.0479$ and for the anisotropic model (ii) $\ln Z(q) = 1.0535$. Figure 5 plots C_{LL} against $1/L$ for the square lattice models. Both of the curves are clearly converging toward zero as expected. For the isotropic model, the curve is approximately linear, with

$$C_{LL} = 0.04L^{-1} \tag{3.9}$$

The results are less clear for the anisotropic model, but still compatible with (3.7).

APPENDIX: THE PARTITION FUNCTIONS

We have calculated the partition functions from Section 2 for all values of L and M in the range $1 \leqslant L, M \leqslant 6$, and all values of h and v. Electronic and hard copies are available on request from the first author. Here we present only the square lattice nonskewed partition functions for $L = 1,..., 5$. It is convenient to divide each of them by a factor of 3^L and (using our earlier remarks) to exhibit them as polynomials in $y = 3x + 3 + 1/x$, so we actually present

$$P_{LL}(y) = 3^{-L} Z_{LL}(y) \tag{A1}$$

We have

$$P_{11}(y) = 3 + 2y + y^2$$

$$P_{22}(y) = 243 + 648y + 324y^2 - 72y^3 + 534y^4 - 184y^5 + 92y^6 - 8y^7 + y^8$$

$$\begin{aligned}P_{33}(y) = {} & 177147 + 1062882y + 2302911y^2 \\ & + 2047032y^3 + 1377810y^4 + 2913084y^5 \\ & + 3158028y^6 + 664848y^7 + 103518y^8 + 930852y^9 \\ & + 306666y^{10} - 270864y^{11} + 220374y^{12} \\ & - 62532y^{13} + 16956y^{14} - 2160y^{15} + 297y^{16} - 18y^{17} + y^{18}\end{aligned}$$

$$\begin{aligned}P_{44}(y) = {} & 1162261467 + 12397455648y + 55788550416y^2 \\ & + 136372012128y^3 + 214315274952y^4 + 324629671968y^5 \\ & + 582654906288y^6 + 750632777568y^7 + 607521384972y^8 \\ & + 795120766560y^9 + 965737104624y^{10} + 130605470496y^{11} \\ & + 322442584488y^{12} + 916063289568y^{13} - 526868886960y^{14} \\ & + 147997956384y^{15} + 596145500838y^{16} - 737714208096y^{17} \\ & + 610533631440y^{18} - 343154709792y^{19} + 156664410984y^{20} \\ & - 55836596448y^{21} + 16860264048y^{22} - 4098594336y^{23} \\ & + 856735500y^{24} - 143074912y^{25} + 20606608y^{26} \\ & - 2274208y^{27} + 217560y^{28} - 14816y^{29} + 880y^{30} - 32y^{31} + y^{32}\end{aligned}$$

$$\begin{aligned}P_{55}(y) = {} & 68630377364883 + 1143839622748050y + 8578797170610375y^2 \\ & + 38127987424935000y^3 + 114511055566221450y^4 \\ & + 268776892687508460y^5 + 589388078205374850y^6 \\ & + 1246116772225702800y^7 + 2209159127195440650y^8 \\ & + 3194839081210230900y^9 + 4647346048981897830y^{10} \\ & + 7079557052341783800y^{11} + 8225530257835830150y^{12} \\ & + 7279248720513503700y^{13} + 9357732890461402200y^{14} \\ & + 11647930212445937760y^{15} + 5762094309484412175y^{16} \\ & + 3517524430230368250y^{17} + 9571985653589609175y^{18} \\ & + 4023612873756685800y^{19} - 2229800910702224940y^{20}\end{aligned}$$

$$+4898159054026700400y^{21}+2681786734169855850y^{22}$$
$$-3147689863270981800y^{23}+2051627825339895150y^{24}$$
$$+1388963485815183972y^{25}-2128929001082085150y^{26}$$
$$+1331521145545374000y^{27}+576842251911190300y^{28}$$
$$-746264103632814600y^{29}+794712829019154840y^{30}$$
$$-530326171478212200y^{31}+272216641223522475y^{32}$$
$$-112688467988737950y^{33}+39181982508236025y^{34}$$
$$-11549532336644520y^{35}+2939341744610550y^{36}$$
$$-645489038603700y^{37}+123764044894650y^{38}$$
$$-20572630471200y^{39}+2994872555520y^{40}$$
$$-376168331200y^{41}+41274998450y^{42}-3850715800y^{43}$$
$$+311887300y^{44}-20890960y^{45}+1201800y^{46}-54000y^{47}$$
$$+2025y^{48}-50y^{49}+y^{50}$$

REFERENCES

1. T. D. Lee and C. N. Yang, *Phys. Rev.* **87**:404–409, 410–419 (1952).
2. R. B. Potts, *Proc. Camb. Phil. Soc.* **48**:106 (1952).
3. F. Y. Wu, *Rev. Mod. Phys.* **54**:235 (1982).
4. R. J. Baxter, *J. Phys. A* **20**:5241–5261 (1987).
5. P. P. Martin and J. M. Maillard, *J. Phys. A* **19**:L547–L551 (1986).
6. P. P. Martin, *Nucl. Phys. B* **225**:497–504 (1983).
7. P. Martin, *Potts Models and Related Problems in Statistical Mechanics* (World Scientific, Singapore, 1991).
8. R. J. Baxter, *J. Stat. Phys.* **28**:1–41 (1982).
9. R. J. Baxter, *J. Phys. C* **6**:L445–L448 (1973).
10. G. Albertini, S. Dasmahapatra, and B. M. McCoy, *Int. J. Mod. Phys. A* **7**(Suppl. 1A):1 (1992).
11. R. Kedem and B. M. McCoy, *J. Stat. Phys.* **71**:865–901 (1993).
12. J. L. Cardy, Conformal invariance and statistical mechanics, in *Les Houches, Session XLIV, Fields, Strings and Critical Phenomena*, E. Brézin and J. Zinn-Justin, eds. (1989).
13. R. J. Baxter, J. H. H. Perk, and H. Au-Yang, *Phys. Lett. A* **128**:138–142 (1988).
14. R. J. Baxter, V. V. Bazhanov, and J. H. H. Perk, *Int. J. Mod. Phys. B* **4**:803–870 (1990).
15. V. A. Fateev and A. B. Zamolodchikov, *Phys. Lett. A* **92**:37–39 (1982).
16. M. Kashiwara and T. Miwa, *Nucl. Phys. B* **275**:121–134 (1986).
17. R. J. Baxter, *Exactly Solved Models in Statistical Mechanics* (Academic Press, London, 1982).
18. D. E. Knuth, *The Art of Computer Programming*, Vol. 2—*Semi-Numerical Algorithms* (Addison-Wesley, Reading, Massachusetts, 1969).
19. B. M. McCoy and T. T. Wu, *The Two-Dimensional Ising Model* (Harvard University Press, Cambridge, Massachusetts, 1973).

20. P. A. Pearce, *Int. J. Mod. Phys. B* **4**:715–734 (1990).
21. P. Christe and M. Henkel, *Introduction to Conformal Invariance and Its Applications to Critical Phenomena* (Springer-Verlag, Berlin, 1993).
22. J. L. Cardy, in *Phase Transitions and Critical Phenomena*, Vol. 11, C. Domb and J. L. Lebowitz, eds. (Academic Press, London, 1987).
23. C. Itzykson, in *Proceedings First Asia Pacific Workshop on High Energy Physics*, B. E. Baaquie, C. K. Chew, C. H. Oh, and K. K. Phua, eds. (World Scientific, Singapore, 1987).
24. L. P. Kadanoff, W. Goetze, D. Hamblen, R. Hecht, E. A. S. Lewis, V. V. Palciauskas, M. Rayl, and J. Swift, *Rev. Mod. Phys.* **39**:395–431 (1967).
25. A. A. Belavin, A. M. Polyakov, and A. B. Zamolodchikov, *Nucl. Phys. B* **241**:333–380 (1984).
26. A. Cappelli, C. Itzykson, and J.-B. Zuber, *Nucl. Phys. B* **280**:445–465 (1987).
27. D. Friedan, Z. Qiu, and S. Shenker, *Phys. Rev. Lett.* **52**:1575–1578 (1984); in *Vertex Operators in Mathematics and Physics*, J. Lepowsky, S. Mandelstam, and I. Singer, eds. (Springer, New York, 1985).
28. Vl. S. Dotsenko, *Nucl. Phys. B* **235**:54–74 (1984).